Eur Radiol (2011) 21:385–392
DOI 10.1007/s00330-010-1926-0

UROGENITAL

Dual-energy CT with tin filter technology for the discrimination of renal lesion proxies containing blood, protein, and contrast-agent. An experimental phantom study

Christoph Karlo · Arno Lauber · Robert Paul Götti · Stephan Baumüller · Paul Stolzmann · Hans Scheffel · Lotus Desbiolles · Bernhard Schmidt · Borut Marincek · Hatem Alkadhi · Sebastian Leschka

Received: 14 June 2010 / Revised: 25 July 2010 / Accepted: 4 August 2010 / Published online: 15 August 2010

Abstract
Purpose To differentiate proxy renal cystic lesions containing protein, blood, iodine contrast or saline solutions using dual-energy CT (DECT) equipped with a new tin filter technology (TFT).
Materials and methods 70 proxies (saline, protein, blood and contrast agent) were placed in unenhanced and contrast-enhanced kidney phantoms. DECT was performed at 80/140 kV with and without tin filtering. Two readers measured the CT attenuation values in all proxies twice. An 80/140 kV ratio was calculated.
Results All intra- and interobserver agreements were excellent (r=0.93–0.97; p<0.001). All CT attenuation values were significantly higher in the enhanced than in the unenhanced setting (p<0.05; average increase, 12.5±3.6HU), while the ratios remained similar (each, p>0.05). The CT attenuation of protein, blood and contrast agent solution differed significantly with tin filtering (p<0.01–0.05). Significant differences were found between the ratios of protein and blood compared to contrast medium solution (each, p<0.05) and between the ratios of protein and blood in both phantoms with tin filtering (each, p<0.05).
Conclusion DECT allows discrimination between a proxy renal lesion containing contrast agent and lesions containing protein and blood through their different attenuation at 80 kV and 140 kV. Further discrimination between protein and blood containing proxies is possible when using a tin filter.

Keywords Dual-energy CT · DECT · Renal cysts · Kidney lesions · Tin filter

C. Karlo (✉) · A. Lauber · R. P. Götti · S. Baumüller · P. Stolzmann · H. Scheffel · L. Desbiolles · B. Marincek · H. Alkadhi · S. Leschka
Institute for Diagnostic Radiology, University Hospital Zurich, Raemistrasse 100,
8091 Zurich, Switzerland
e-mail: christoph.karlo@usz.ch

B. Schmidt
Siemens Healthcare,
Forchheim, Germany

H. Alkadhi
Cardiac MR PET CT Group,
Massachusetts General Hospital and Harvard Medical School,
Boston, MA, USA

Introduction

Cystic renal lesions are estimated to be present in 20–40% of the population and represent frequent, most of the times incidental findings in abdominal computed tomography (CT) examinations [1]. Alongside the cyst's diameter, wall thickness, presence of septa and contrast enhancing components, the measurement of the mean CT attenuation value (in Hounsfield Units, HU) of the cysts' content on unenhanced CT images as well as the assessment of its attenuation pattern after the administration of intravenous contrast media are supporting the radiologists to classify cystic renal lesions [2]. Cysts surrounded by thin, smooth walls and mean CT attenuation values between 0 and 20 HU are considered simple benign cysts if they do not enhance after the application of contrast agents [2–4]. These cysts are classified category I by Bosniak [1]. Homogeneous cysts with mean CT attenuation values between 40 and 90 HU on unenhanced CT images are considered hyperattenuating cysts if they are also enclosed by thin, smooth walls and

do not enhance after contrast agent administration [3]. Cysts containing blood (i.e. haemorrhagic cysts) or protein (i.e. proteinaceous cysts) also represent as hyperattenuating cystic renal lesions on unenhanced CT examinations [5, 6]. In general, cystic renal lesions measuring between 20 and 40 HU may be considered proteinaceous cysts. In case of attenuation values of 40–50 HU the lesions content may be of haemorrhagic origin [7]. These homogeneously hyperattenuating, non-enhancing cystic renal lesions are considered benign and classified category II by Bosniak [1]. Therefore follow-up CT examinations are not required.

On contrast-enhanced single-energy CT images, haemorrhagic or proteinaceous contents as well as contrast enhancement may be responsible for an increase in attenuation value of a cystic renal lesion's content. However, unless additional unenhanced CT is performed, contrast agent uptake cannot be determined or ruled-out reliably. Furthermore, the differentiation between haemorrhagic and proteinaceous cystic renal lesions is currently not possible with standard, single-energy CT acquisition techniques [5, 7]. However, this differentiation might be of interest in order to differentiate renal cell carcinomas from haemorrhagic or inflammatory renal cysts.

The purpose of this study was to assess the performance of dual-energy CT (DECT) equipped with a new tin filter technology to differentiate renal cyst proxies containing protein, blood, iodinated contrast agent or saline solution in an experimental phantom study setup.

Materials and methods

Kidney phantom

A hollow acrylic elliptic sphere (120×65×65 mm) served as a kidney phantom. In a first benchmark model, the phantom was filled with minced beef mixed with distilled water to simulate unenhanced renal parenchyma (unenhanced kidney phantom). In a second benchmark model, the phantom was filled with minced beef mixed with iodinated contrast agent (Ultravist, 300 mg iodine/mL, Bayer Schering Pharma, Berlin, Germany) to a mean CT attenuation of 250 HU as measured at 120 kV single-energy CT to simulate contrast-enhanced renal parenchyma in the nephrographic phase (contrast-enhanced kidney phantom).

Cystic renal lesion proxies

Seventy spherical proxies were manufactured from rubber gloves and randomly filled with either sterile saline, fresh human blood, bovine serum albumine or iodinated contrast agent solutions:

- 10 proxies filled with sterile saline solution resulting in a mean CT attenuation value of 0 HU simulating simple renal cysts;
- 20 proxies filled with iodinated contrast medium (Ultravist, 300 mg iodine/mL, Bayer Schering Pharma, Berlin, Germany) titrated with distilled water to concentrations of 0.9 mg (n=10) and 1.8 mg (n=10) iodine/ml and mean CT attenuation values of 20 and 40 HU simulating renal mass lesions with different degrees of attenuation;
- 20 proxies filled with bovine serum albumine (Cohn Fraction V, ≥96% purified lyophilized powder, Sigma Aldrich Co., St. Louis MO, USA) titrated with distilled water to mean CT attenuation values of 20 and 40 HU simulating proteinaceous renal cysts with different degrees of attenuation;
- 20 proxies filled with fresh human blood titrated with distilled water to mean CT attenuation values of 20 and 40 HU simulating complicated haemorrhagic renal cysts with different degrees of attenuation.

The CT attenuation of all titrated solutions was determined by mean CT attenuation value measurements upon single-energy CT images of each lesion proxy in the kidney phantom using the following CT acquisition parameters: collimation 64×0.6 mm, slice acquisition 128×0.6 mm by means of a z-flying focal spot, tube voltage 120 kV, tube current-time product 200 mAs, pitch 0.35, and rotation time 0.33 s. Images of this acquisition were reconstructed to a slice thickness of 1.0 mm at a reconstruction increment of 0.7 mm using a standard soft tissue convolution kernel (B30f).

Experimental setup

Each ten cystic renal lesion proxies titrated to different CT attenuation values (i.e. 20 HU and 40 HU) were randomly placed inside the kidney phantom ensuring that each proxy was completely surrounded by minced beef and was neither in contact with another proxy nor with the wall of the phantom. A radiologist not involved in data analysis noted the position of each renal proxy and its content. The assembled kidney phantom was submerged in a 28-cm tank filled with distilled water to simulate surrounding body attenuation. The water tank was then examined using a second-generation 128-slice dual-source CT system (SOMATOM Definition Flash, Siemens Healthcare, Forchheim, Germany) operated using two different protocols:

Protocol A: Tube voltage pair of 140 kV and 80 kV with tube current time products of 56 mAs and 308 mAs, respectively, no tin filtering.

Protocol B: Tube voltage pair of 140 kV and 80 kV with tube current time products of 140 mAs and 333 mAs and tin filtering of the 140 kV tube.

For DECT, the tube currents were adjusted to yield constancy in CT volume dose index of 9.0 mGy for both protocols. The CT acquisition parameters were: collimation, 32×0.6 mm, slice acquisition, 64×0.6 mm by means of a z-flying focal spot, pitch, 0.35, and gantry rotation time, 0.5 s. All image data was reconstructed to a slice thickness of 1.0 mm at a reconstruction increment of 0.7 mm using a soft tissue convolution kernel specifically designed for DECT (D30).

All images of the DECT acquisitions of the unenhanced and contrast-enhanced phantom were reformatted displaying only a single proxy at a time for both protocols (i.e. with and without tin-filtering) and energy spectra (i.e. 80 kV and 140 kV). All text annotations were removed from all images by a radiologist not involved in data analysis.

CT data analysis

A radiologist not involved in further data analysis measured the size of each lesion proxy using an electronic calliper tool. The anonymised dual-energy images were displayed in random order to two radiologists experienced in genitourinary imaging. Both observers (Reader 1, R1, 4 years of genitourinary cross-sectional image interpretation experience; and Reader 2, R2, 3 years of experience) were blinded to each other and independently performed a quantitative analysis of the CT attenuation values by placing a region of interest inside each proxy. Each observer repeated the measurement within a time interval of 2 weeks in a second data analysis session. The standard deviation of the mean CT attenuation value in each lesion was noted and considered to define image noise.

Statistical analysis

All statistical analysis was performed using commercially available software (SPSS, release 17.0, Chicago, IL, USA). A p-level < 0.05 was considered to indicate statistical significance.

Categorical variables were expressed as frequencies and percentages. Numerical variables were expressed as means±standard deviations. Kruskal Wallis analysis was performed to test for differences in lesion proxy size among the different groups. Inter- and intra-observer agreements concerning measurement of CT attenuation values within the lesion proxies were assessed using Pearson's analysis. The ratio of the mean CT attenuation values between 80 kV and 140 kV (i.e. 80/140 ratio; DE-Ratio) was calculated for each setting. CT attenuation values and DE-ratios were statistically compared using the Wilcoxon paired-sample test.

Results

Cystic renal lesion proxies' characteristics

The average size of all lesion proxies (i.e. 20±3 mm; range, 14–28 mm) was similar (p=0.29) for different concentrations (i.e. 20 HU and 40 HU) and contents.

Intraobserver and interobserver agreements

Intra- (R1, r=0.97; p<0.001; R2, r=0.95; p<0.001) and interobserver (r=0.93; p<0.001) agreements for all CT attenuation value measurements were excellent. Thus, the average of CT attenuation value measurements of both readers and both image analysis sessions were used for further statistical analysis.

Quantitative measurements of the proxies' contents

A summary of the quantitative analysis of the CT attenuation values in both protocols (i.e. with and without tin filtering) and kidney phantoms (i.e. contrast-enhanced and unenhanced) is provided in Tables 1 and 2.

Comparison of results between both phantoms

In the contrast-enhanced phantom, all CT attenuation values were significantly higher than in the unenhanced phantom (average increase, 12.5±3.6 HU; p<0.05) in both energy spectra (i.e. 80 kV and 140 kV) with and without tin filtering. There was no significant difference in DE-ratios of the protein-, blood-, and contrast-containing proxies between the two phantoms (each, p>0.05).

Unenhanced kidney phantom

Comparing protein-, blood-, and contrast-containing proxies, the CT attenuation values were significantly different at 140 kV (each, p<0.01) and 80 kV (each, p<0.05), with and without tin filtering (Fig. 1).

There was a significant difference of the CT attenuation values of protein-, blood-, and contrast-containing proxies between 80 kV and 140 kV with tin filtering (each, p<0.05) and for contrast-containing proxies without tin filtering (p<0.01), while no significant difference was found for protein- (p=0.74) and blood-containing proxies (p=0.38) without tin filtering between 80 kV and 140 kV. With the use of a tin filter, the DE-ratios were significantly different for protein-containing proxies (p<

Table 1 Quantitative analysis of the proxies' CT attenuation values in the *unenhanced* kidney phantom

	[a]N_{CT} 120kV	Protocol A—tin filter OFF			Protocol B—tin filter ON			*p* values[c]
		[a]N_{CT} 80kV	[a]N_{CT} 140kV	Ratio $_{80/140}$	[a]N_{CT} 80kV [b]SN	[a]N_{CT} 140kV SN	Ratio $_{80/140\ SN}$	
Saline	0	2.5±1.7	2.5±1.1	1.1±1.1	2.1±2.1	2.5±1.8	1.2±0.8	0.72
Protein	20	16.9±1.4	16.8±1.5	1.0±0.1	14.3±2.4	18.4±1.3	0.8±0.1	<0.01
	40	39.0±1.4	38.8±1.7	1.0±0.1	34.9±2.5	43.7±2.0	0.8±0.1	<0.01
Blood	20	20.0±1.1	18.3±2.8	1.1±0.2	21.7±1.9	17.5±1.2	1.2±0.1	0.12
	40	35.9±2.0	33.5±2.1	1.1±0.1	37.7±3.3	33.7±2.3	1.1±0.1	0.38
Contrast medium	20	25.2±1.4	12.0±1.0	2.1±0.2	20.9±1.4	10.7±0.8	2.0±0.2	0.48
	40	46.5±1.5	24.1±2.0	2.0±0.1	42.3±2.2	18.8±1.3	2.2±0.3	0.06

[a] CT attenuation value measurement in Hounsfield units (HU)

[b] SN = tin filter

[c] *p* values are derived from statistical comparison of the different ratios between CT attenuation values measured at 80 kV and 140 kV between protocol A and protocol B (*Wilcoxon paired sample test*)

0.01, Table 1) when compared to the non-tin filtered acquisition.

Contrast-enhanced kidney phantom

The CT attenuation values of protein-, blood-, and contrast-containing proxies were significantly different at 80 kV (each, $p<0.05$) and 140 kV (each, $p<0.01$, Fig. 1), with and without tin filtering.

There was a significant difference of the CT attenuation values between 80 kV and 140 kV for protein-, blood-, and contrast-containing proxies with tin filtering (each, $p<0.01$) as well as for contrast-containing proxies without tin filtering ($p<0.01$). No significant difference was found for protein- ($p=0.21$) and blood-containing proxies ($p=0.08$) between 80 kV and 140 kV. With and without tin filtering, the DE-ratios were significantly different for protein-containing proxies ($p<0.01$, Table 2).

Image noise

The image noise was significantly lower in the tin-filtered acquisitions (16±1 HU) when compared to the non-tin-filtered acquisitions (18±1 HU; $p<0.05$).

Discrimination of protein, blood and contrast agent

Without the application of tin filtering, the DE-ratios for protein- and blood-containing proxies were significantly different from the DE-ratios of contrast containing proxies in the unenhanced (Fig. 2a) and contrast-enhanced phantom (each, $p<0.05$; Fig. 2b). There was no significant difference in the DE-ratios between protein- and blood-containing proxies in the unenhanced ($p=0.79$; Fig. 2a) and contrast-enhanced kidney phantom ($p=0.29$; Fig. 2b).

With the application of tin filtering, the DE-ratios for protein- and blood-containing proxies were significantly

Table 2 Quantitative analysis of the proxies' CT attenuation values in the contrast enhanced kidney phantom

	[a]N_{CT} 120kV	Protocol A—Tin Filter OFF			Protocol B—Tin Filter ON			*p* values[c]
		[a]N_{CT} 80kV	[a]N_{CT} 140kV	Ratio $_{80/140}$	[a]N_{CT} 80kV [b]SN	[a]N_{CT} 140kV SN	Ratio $_{80/140\ SN}$	
Saline	0	12.2±2.8	10.8±2.7	1.1±0.2	13.1±2.9	10.8±3.8	1.2±0.5	0.53
Protein	20	32.9±6.4	32.9±5.9	1.0±0.1	22.4±2.6	31.3±5.0	0.7±0.1	<0.01
	40	48.8±2.8	51.0±2.0	1.0±0.1	41.9±3.0	50.2±5.9	0.8±0.1	<0.01
Blood	20	33.7±4.8	28.9±3.3	1.2±0.2	34.4±2.8	25.4±3.1	1.4±0.1	0.07
	40	51.0±4.8	44.2±4.0	1.2±0.1	49.3±3.3	37.9±3.6	1.3±0.1	0.23
Contrast medium	20	45.9±6.0	23.2±2.0	2.0±0.3	36.9±3.9	18.4±3.0	2.0±0.2	0.47
	40	59.5±2.6	31.9±2.2	1.9±0.2	57.7±2.6	27.5±1.9	2.1±0.2	0.19

[a] CT attenuation value measurement in Hounsfield units (HU)

[b] SN = tin filter

[c] *p* values are derived from statistical comparison of the different ratios between CT attenuation values measured at 80 kV and 140 kV between protocol A and protocol B (*Wilcoxon paired sample test*)

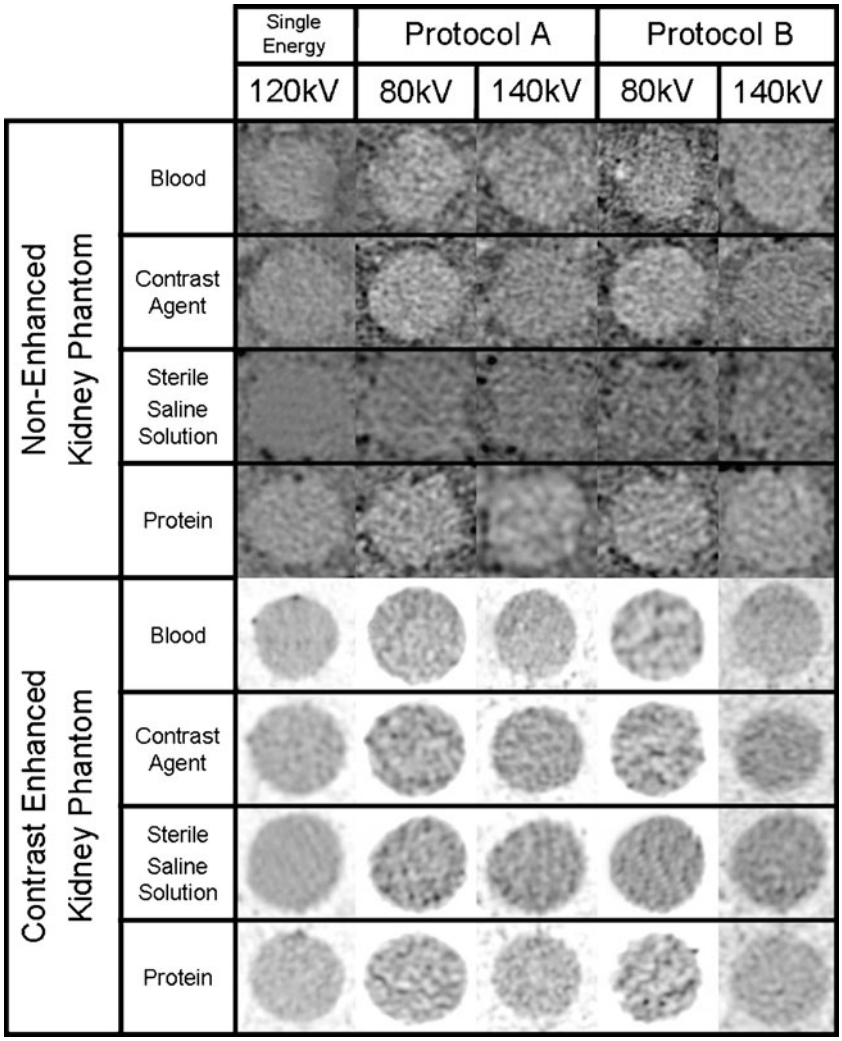

Fig. 1 Imaging examples of renal cyst proxies containing blood, contrast media, saline solution, and protein at single-energy CT (120 kV) and dual-energy CT with and without tin filtering in the unenhanced and contrast-enhanced kidney phantom. Note the difference in attenuation of the cysts and the contrast-enhanced minced beef at the various X-ray energy spectra

different from the DE-ratios of contrast containing proxies in the unenhanced (Fig. 2c) and contrast-enhanced kidney phantom (each, $p<0.05$; Fig. 2d). The DE-ratios between protein- and blood-containing proxies were significantly different in the unenhanced ($p<0.05$; Fig. 2c) and contrast-enhanced kidney phantom ($p<0.05$; Fig. 2d).

Discussion

The purpose of this study was to discriminate cystic renal lesion proxies with different contents using DECT with a new tin filtering technology. Our results have shown, that a differentiation between contrast material containing cystic renal lesion proxies and protein- or blood-containing cystic renal lesion proxies is feasible using 80/140 kV ratios calculated from DECT data. Further on we were able to discriminate protein- from blood containing cystic renal lesion proxies by using an additional tin filter.

In the early 1970s, DECT had been introduced for material decomposition making use of attenuation characteristics of different materials at two different X-ray energy spectra [8]. The recent introduction of dual-source CT (DSCT) systems has re-enlivened DECT for various clinical indications [9–17], owing to the simultaneous data acquisition of two X-ray tube-detector systems at two different X-ray spectra.

Common applications of DECT include the reconstruction of virtual unenhanced images to spare the (true) unenhanced CT acquisition and therefore reduce the total radiation dose [9–12], the detailed use of material decomposition techniques to characterise urinary stones of different compositions [9, 13–16], the separation of xenon from air [18], or blood from air [19, 20].

Recently, the second generation of DSCT systems—equipped with a new tin filter technology for increased X-ray energy spectra separation [17]—was introduced. These tin filters, mounted on the 140 kV tube, have been suggested, but not proven to further improve the differentiation of material sharing overlapping attenuation values at single-

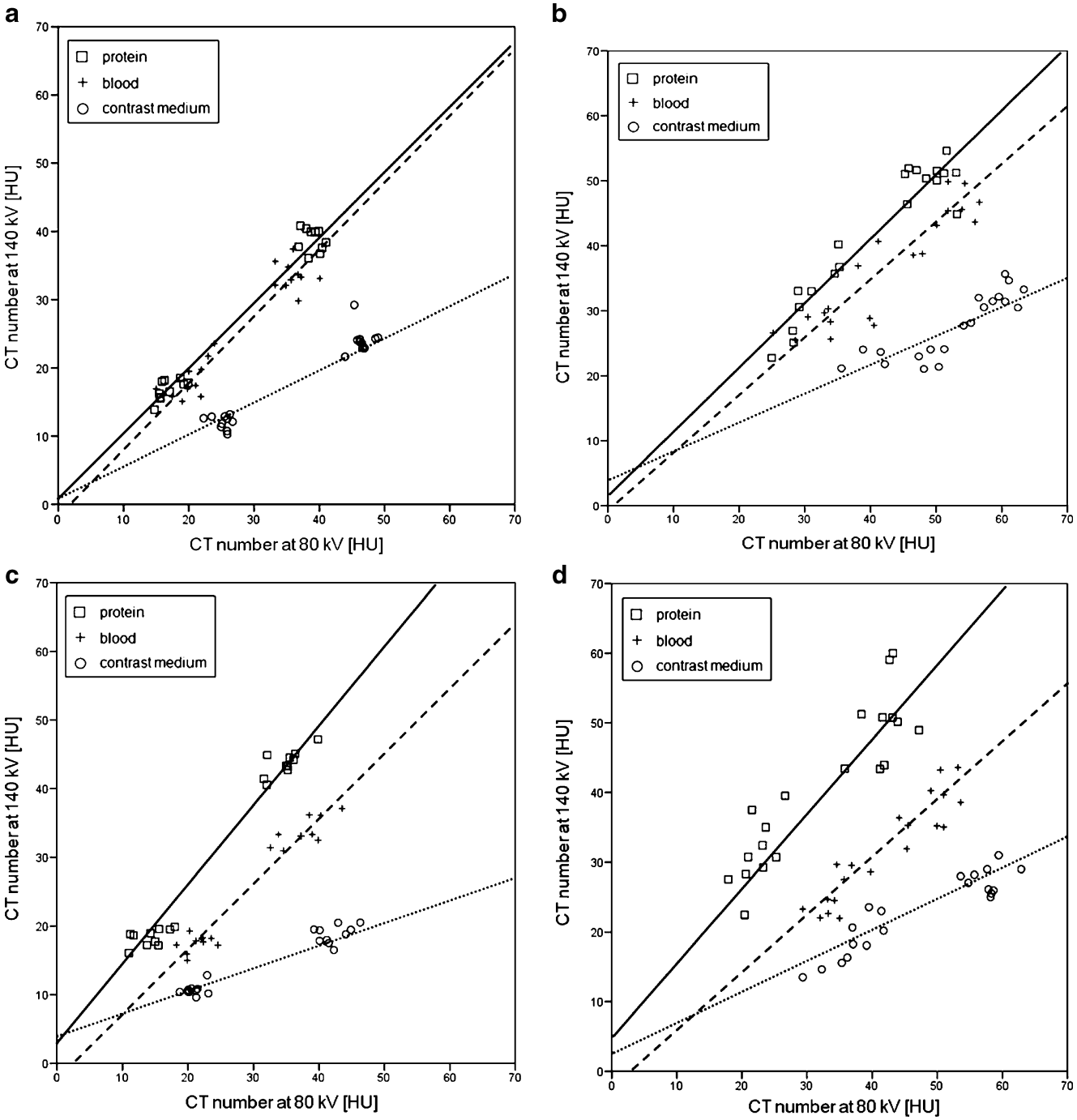

Fig. 2 Dual-energy ratio of the CT attenuation value at 80 kV/140 kV for protein, blood, and contrast-containing lesion proxies without tin filtering in the unenhanced (**a**) and contrast-enhanced kidney phantom (**b**); and with tin filtering in the unenhanced (**c**) and contrast-enhanced kidney phantom (**d**). With and without tin filtering, the 80/140 kV ratios of protein and blood-containing proxies were significantly different from that of the contrast-containing proxies in the unenhanced and contrast-enhanced kidney phantom (each, $p<0.05$). Without tin filtering (**a**,**b**), there was no significant difference in the 80/140 kV ratios between protein and blood-containing lesions, while the 80/140 kV ratios were significantly different with the application of the tin filter (**c**,**d**)

energy CT examinations. Very recently an improved differentiation of urinary calculi has been reported using tin filtered dual-energy CT [21, 22]. Additionally, Leschka et al. were able to differentiate renal cysts from contrast-enhancing renal mass lesions by applying the tin filter technology to dual-energy CT [23] and Graser et al. have reported an added value of tin-filtered DECT when determining the dignity of renal lesions [24].

The classification of renal cysts using abdominal CT primarily relies on their attenuation behaviour on unen-

hanced images and on their enhancement pattern after the administration of intravenous iodinated contrast agent. However, most cystic renal lesions are discovered incidentally on contrast-enhanced abdominal CT examinations performed for non-renal indications [1] and in case of equivocal findings regarding their attenuation on contrast-enhanced CT studies, patients may need to be recalled to undergo a second, unenhanced abdominal CT, a procedure causing increased costs and radiation exposure to the patient. Moreover, the assessment of enhancement of cystic renal lesions may be prone to errors by erroneously assuming a "true" enhancement in the presence of the—so called—pseudoenhancement, which refers to an artificial increase in attenuation of a simple renal cyst following contrast agent application, and is most problematic for small cysts at high levels of renal parenchymal enhancement [8, 9]. This issue is further complicated by the fact that certain renal cell carcinomas may enhance in a rather weak and homogeneous manner [25]. Pseudoenhancement thus may lead to mischaracterization of a small renal cyst as a neoplasm eventually leading to unnecessary interventions. We found higher CT attenuation values in the contrast-enhanced kidney phantom compared to the unenhanced phantom, due to this pseudoenhancement. Interestingly, the dual-energy ratios for blood-, protein-, and contrast-containing cystic renal lesion proxies were similar in both phantoms.

The principle of DECT bases on the varying attenuations of different materials at two different X-ray energy spectra [9–11, 13–15, 17]. In a recent study, the ability of DECT (without tin filter technology) to discriminate renal cysts from iodine containing renal masses was shown, with a sensitivity of 97% and specificity of 83% [26]. Our study confirms and extends those results by demonstrating the feasibility of DECT to differentiate proteinaceous or haemorrhagic from contrast containing cystic renal lesion proxies by means of their different attenuation behaviour at 140 kV and 80 kV. We found that the DE-ratios of protein- or blood-containing proxies differ significantly from the DE-ratios of contrast-containing proxies. Consequently, DECT allows for the discrimination of protein- or blood-containing cystic renal lesion proxies from contrast-containing proxies. Therefore, additional unenhanced CT need not be performed. Our study also demonstrates that a further discrimination between proteinaceous and haemorrhagic proxies is feasible when applying a tin filter. Without this tin filter, a substantial overlap in the CT attenuation values measured at 140 kV and 80 kV was found between protein- and blood-containing proxies. This may be explained by the suboptimal separation of X-ray energy spectra without the use of a tin filter which is particularly important for material with only minor differences in X-ray absorption [14]. The tin filter reduces overlap in X-ray energy spectra by increasing the mean photon energy of the 140 kV-tube and, therefore, improves both material differentiation and decomposition [17]. As a matter of fact, we found different DE-ratios between the attenuation values measured at 140 kV and 80 kV for proteinaceous cysts with or without the application of the tin filter. Consequently, a significantly different DE-ratio between protein- and blood-containing proxies was found in the protocol applying the tin filter allowing for the discrimination of these contents.

Albeit the phantom used in our study was designed to simulate optimal conditions comparable to in-vivo abdominal CT, we have to acknowledge some limitations. This is a phantom study, and therefore the performance of DECT for discriminating protein, blood, and lesions containing contrast agent needs to be validated in further clinical studies. Furthermore, we assumed albumin to be the main component in proteinaceous renal cysts. The real content of proteinaceous cysts might vary from patient to patient and may depend on a possible underlying pathology. Therefore, the DE-ratios in clinical abdominal CT might differ from our results, and a larger overlap of the CT attenuation values measured at 140 kV and 80 kV between protein and blood content might limit the discrimination of proteinaceous and haemorrhagic cysts in clinical practice. However, we have chosen albumin because it is highly available in purified condition, and, therefore, easy to handle in experimental settings. Another limitation may be the size of the kidney phantom. With a diameter of 28 cm, a comparison to human bodies is not possible. The attenuation values of cystic renal lesions may vary in vivo. Another option for dual-energy CT in vivo is the use of a 140 kV/100 kV protocol, which may be helpful especially in obese patients.

Conclusion

In conclusion, DECT is able to discriminate proteinaceous or haemorrhagic cystic renal lesion proxies from cystic renal lesion proxies containing contrast agent through their different attenuation behaviour at 140 kV and 80 kV. Applying the tin filter technology to DECT allows for a further discrimination of protein and blood content within the cystic renal lesion proxies.

References

1. Tada S, Yamagishi J, Kobayashi H, Hata Y, Kobari T (1983) The incidence of simple renal cyst by computed tomography. Clin Radiol 34:437–439
2. Bosniak MA (1986) The current radiological approach to renal cysts. Radiology 158:1–10
3. Bosniak MA (1991) The small (less than or equal to 3.0 cm) renal parenchymal tumor: detection, diagnosis, and controversies. Radiology 179:307–317

4. Israel GM, Bosniak MA (2005) How I do it: evaluating renal masses. Radiology 236:441–450
5. Jonisch AI, Rubinowitz AN, Mutalik PG, Israel GM (2007) Can high-attenuation renal cysts be differentiated from renal cell carcinoma at unenhanced CT? Radiology 243:445–450
6. Silverman SG, Mortele KJ, Tuncali K, Jinzaki M, Cibas ES (2007) Hyperattenuating renal masses: etiologies, pathogenesis, and imaging evaluation. Radiographics 27:1131–1143
7. Silverman SG, Israel GM, Herts BR, Richie JP (2008) Management of the incidental renal mass. Radiology 249:16–31
8. Millner MR, McDavid WD, Waggener RG, Dennis MJ, Payne WH, Sank VJ (1979) Extraction of information from CT scans at different energies. Med Phys 6:70–71
9. Chandarana H, Godoy MC, Vlahos I et al (2008) Abdominal aorta: evaluation with dual-source dual-energy multidetector CT after endovascular repair of aneurysms—initial observations. Radiology 249:692–700
10. Scheffel H, Stolzmann P, Frauenfelder T et al (2007) Dual-energy contrast-enhanced computed tomography for the detection of urinary stone disease. Invest Radiol 42:823–829
11. Stolzmann P, Frauenfelder T, Pfammatter T et al (2008) Endoleaks after endovascular abdominal aortic aneurysm repair: detection with dual-energy dual-source CT. Radiology 249:682–691
12. Chae EJ, Song JW, Seo JB, Krauss B, Jang YM, Song KS (2008) Clinical utility of dual-energy CT in the evaluation of solitary pulmonary nodules: initial experience. Radiology 249:671–681
13. Fletcher JG, Takahashi N, Hartman R et al (2009) Dual-energy and dual-source CT: is there a role in the abdomen and pelvis? Radiol Clin North Am 47:41–57
14. Graser A, Johnson TR, Chandarana H, Macari M (2009) Dual energy CT: preliminary observations and potential clinical applications in the abdomen. Eur Radiol 19:13–23
15. Stolzmann P, Scheffel H, Rentsch K et al (2008) Dual-energy computed tomography for the differentiation of uric acid stones: ex vivo performance evaluation. Urol Res 36:133–138
16. Stolzmann P, Kozomara M, Chuck N et al (2009) In vivo identification of uric acid stones with dual-energy CT: diagnostic performance evaluation in patients. Abdominal imaging. doi:10.1007/s00261-009-9569-9
17. Primak AN, Ramirez Giraldo JC, Liu X, Yu L, McCollough CH (2009) Improved dual-energy material discrimination for dual-source CT by means of additional spectral filtration. Med Phys 36:1359–1369
18. Chae EJ, Seo JB, Goo HW et al (2008) Xenon ventilation CT with a dual-energy technique of dual-source CT: initial experience. Radiology 248:615–624
19. Ferda J, Ferdova E, Mirka H et al (2009) Pulmonary imaging using dual-energy CT, a role of the assessment of iodine and air distribution. European Journal of Radiology. doi:10.1016/j.ejrad.2009.08.005
20. Thieme SF, Johnson TR, Lee C et al (2009) Dual-energy CT for the assessment of contrast material distribution in the pulmonary parenchyma. AJR 193:144–149
21. Stolzmann P, Leschka S, Scheffel H et al (2010) Characterization of urinary stones with dual-energy CT: improved differentiation using a tin filter. Invest Radiol 45:1–6
22. Thomas C, Krauss B, Ketelsen D et al (2010) Differentiation of urinary calculi with dual energy CT: effect of spectral shaping by high energy tin filtration. Invest Radiol 45:393–398
23. Leschka S, Stolzmann P, Baumuller S et al (2010) Performance of dual-energy CT with tin filter technology for the discrimination of renal cysts and enhancing masses. Acad Radiol 17:526–534
24. Graser A, Becker CR, Staehler M et al (2010) Single-phase dual-energy CT allows for characterization of renal masses as benign or malignant. Invest Radiol 45:399–405
25. Tsuda K, Kinouchi T, Tanikawa G et al (2005) Imaging characteristics of papillary renal cell carcinoma by computed tomography scan and magnetic resonance imaging. Int J Urol 12:795–800
26. Brown CL, Hartman RP, Dzyubak OP et al (2009) Dual-energy CT iodine overlay technique for characterization of renal masses as cyst or solid: a phantom feasibility study. Eur Radiol 19:1289–1295